Framework for Online Optimization of Recombinant Protein Expression in High-Cell-Density *Escherichia coli* Cultures Using GFP-Fusion Monitoring

Hee Jeong Chae,[1,3,*] Matthew P. DeLisa,[1,3] Hyung Joon Cha,[1,3,†] William A. Weigand,[3] Govind Rao,[2,4] William E. Bentley[1,3]

[1]Center for Agricultural Biotechnology, University of Maryland Biotechnology Institute, College Park, Maryland 20742, USA; telephone: 301-405-4321; fax: 301-314-9075; e-mail: bentley@eng.umd.edu
[2]Medical Biotechnology Center, University of Maryland Biotechnology Institute, College Park, Maryland, USA
[3]Department of Chemical Engineering, University of Maryland, College Park, Maryland, USA
[4]Department of Chemical and Biochemical Engineering, University of Maryland at Baltimore County, Baltimore, Maryland, USA

Received 21 July 1999; accepted 5 March 2000

Abstract: A framework for the online optimization of protein induction using green fluorescent protein (GFP)-monitoring technology was developed for high-cell-density cultivation of *Escherichia coli.* A simple and unstructured mathematical model was developed that described well the dynamics of cloned chloramphenicol acetyltransferase (CAT) production in *E. coli* JM105 was developed. A sequential quadratic programming (SQP) optimization algorithm was used to estimate model parameter values and to solve optimal open-loop control problems for piecewise control of inducer feed rates that maximize productivity. The optimal inducer feeding profile for an arabinose induction system was different from that of an isopropyl-β-D-thiogalactopyranoside (IPTG) induction system. Also, model-based online parameter estimation and online optimization algorithms were developed to determine optimal inducer feeding rates for eventual use of a feedback signal from a GFP fluorescence probe (direct product monitoring with 95-minute time delay). Because the numerical algorithms required minimal processing time, the potential for product-based and model-based online optimal control methodology can be realized. © 2000 John Wiley & Sons, Inc. *Biotechnol Bioeng* **69:** 275–285, 2000.

Keywords: green fluorescent protein; chloramphenicol acetyltransferase; high-cell-density cultivation; *Escherichia coli*; mathematical model; online optimization

INTRODUCTION

Metabolic engineering has enabled the exploitation of cellular and energetic pathways of various microorganisms, such as bacteria, yeast, insect, and mammalian cells, in order to produce recombinant proteins. Typically, recombinant cells are grown in reactors employing control algorithms designed to maximize cell productivity. In cases where online measurement sensors for glucose and acetate are available, advanced strategies using feedback from the measurements have been implemented (Kleman et al., 1991; Shimizu et al., 1988; Turner et al., 1994). These strategies control recombinant product formation in an indirect manner, usually via the maximization of biomass or minimization of metabolic byproducts. The productivity of recombinant foreign protein is generally unknown until offline analysis of fermentation samples has been performed. Although many of the critical process parameters cannot currently be measured online, intensive research efforts have been made to develop new sensors and sampling devices/techniques (Schugerl et al., 1996). For example, online monitoring of green fluorescence protein (GFP) fluorescence to determine recombinant product concentration (Randers-Eichhorn et al., 1997), and online monitoring of firefly luciferase to track intracellular ATP concentration (Lasko and Wang, 1996) have been reported. In the case of GFP, green fluorescence could be monitored online and/or in vivo during fermentation to indicate product level (Albano et al., 1996, 1998; Cha et al., 1997, 1999a; DeLisa et al., 1999c; Randers-Eichhorn et al., 1997). Because GFP fluorescence was used to monitor production of a model recombinant protein (CAT) during both low- and high-cell-density cultivations of *E. coli* (DeLisa et al., 1999c), it was suggested that GFP fluorescence could serve as a sensor for taking a process control action.

Importantly, the highly nonlinear nature of biological processes coupled with the extremely slow and inconsistent process dynamics, make process control, particularly model-based control (Lee, 1993), a difficult task. Models

Correspondence to: W. E. Bentley
* *Present affiliation:* Department of Food Technology, Hoseo University, Asan, Korea
† *Present affiliation:* Department of Chemical Engineering, Pohang University of Science and Technology, Pohang, Korea

Contract grant sponsor: U.S. Army; Contract grant number: DAAM01-96-C-0037; Contract grant sponsors: UMCP Bioprocess Scale-Up Facility; Merck; Genentech; Pfizer

for *E. coli*, which are unstructured (fixed cell composition) and nonsegregated (homogeneous population), are computationally simple but often fail during transient conditions or during large and/or rapid perturbations. Dividing a single cell into compartments has allowed generation of models that incorporate details about metabolic mechanisms and pathways (Bentley and Kompala, 1989; Domach and Shuler, 1984); however, these models are computationally complex and many of the state variables are difficult to measure. The inability to measure these states online or at least rapidly offline has excluded these complex models from process control algorithms.

To fully utilize GFP monitoring for optimal control of *E. coli* fermentations, several advances are required: (1) development of online parameter estimator and optimization algorithm that will enable optimization while accommodating the 95-minute time lag associated with GFP chromophore cyclization (Albano et al., 1996); (2) development of a model-based control algorithm that relies on the online estimation and optimization; and (3) coupling of the above mathematical tools with the GFP-based optical measurement probe (Randers-Eichhorn et al., 1997) and the inducer and glucose feed pumps controlling the fermentor.

In this article, we target the first of these requirements. Specifically, we have developed a simple and reliable mathematical model for describing expression of a cloned gene product, CAT, in *E. coli.* Offline and online parameter estimation tools based on a sequential quadratic programming (SQP) otimization algorithm have been developed and are reported. The optimal control problem was solved to obtain an optimal inducer feeding policy to maximize productivity. Then, in situ and in real time, model-based, online parameter estimation and online optimization algorithms were developed, so that the eventual output from a GFP probe could be incorporated. The feasibility of applying online estimation and optimization using GFP is demonstrated via simulation.

MATERIALS AND METHODS

Microorganisms and Media

E. coli strain JM105 (*F′ Δlac-pro thi strA endA sbcB15 hspR4 tra36 pro AB*$^{+}$ *lacI*^{q}*-ZΔM15*) harboring the plasmid pBAD-GFP::CAT (Albano et al., 1998) was used for all batch and fed-batch high-cell-density fermentations. The GFP and CAT genes each possessed a ribosome-binding site (operon fusion) and both were under the control of the P_{BAD} promoter of the *araBAD* (arabinose) operon. *E. coli* strain JM105 bearing the plasmid pTH-GFPuv/CAT (translational fusion) (Cha et al., 1999b) was also used. In this strain, GFP and CAT proteins were expressed as a fusion under the P_{trc} promoter, which is induced by isopropyl-β-D-thiogalactopyranoside (IPTG). A defined medium for high-cell-density experiments using JM105 [pBAD-GFP::CAT] was described by Riesenberg (1991). For the cultivation of JM105 [pTH-GFPuv/CAT], M9 medium with thiamine-HCl (0.166 μg mL^{-1}; Sigma, St. Louis, MO) was used according to Rodriguez and Tait (1983).

Batch and Fed-Batch High-Cell-Density Fermentations

Luria–Bertani (LB) media (100 mL) with ampicillin (100 μg mL^{-1}, Sigma) was used for precultures of *E. coli* in 250-mL Erlenmeyer shake flasks. The cells were grown for 4 h at 30°C in a shaker (New Brunswick Scientific Co., Edison, NJ) at 250 rpm. A portion (5% v/v) of the primary preculture was transferred to defined media (100 mL) with ampicillin (100 μg mL^{-1}) and grown for 12 h at 30°C at 250 rpm.

Batch and fed-batch experiments with *E. coli* JM105 [pBAD-GFP::CAT] and [pTH-GFPuv/CAT] were carried out in a fermentor (Applikon, Foster City, CA) at 30°C, 1 vvm air flow, and 450 rpm stirrer speed, with an initial working volume of 2 L (5% [v/v] inoculum). An Applikon ADI 1030 controller was used to maintain the temperature at 30°C and to control the pH at 6.7 by addition of aqueous NH_4PH (28% v/v). The dissolved oxygen (DO) value was maintained above 30% of air saturation by increasing the agitation rate. To meet the oxygen demand of the cells at the later stages of the high-cell-density cultures, pure oxygen was mixed with the inlet air stream. In addition, sterile filtered antifoam (Sigma) was added when necessary.

E. coli JM105 [pBAD-GFP::CAT] was induced with sterile filtered L-arabinose (0.2%) (Sigma). In the case of JM105 [pTH-GFPuv/CAT], sterile-filtered IPTG was fed exponentially to a final concentration of 1 m*M* along with additional glucose and salts (DeLisa et al., 1999a).

All fed-batch experiments were performed initially with unlimited batch growth lasting until the initial glucose (~18 g L^{-1}) was consumed below 1 g L^{-1}. The substrate feeding strategy was predetermined in all experiments according to the method outlined in Paalme et al. (1990) with a feed solution containing 400 g L^{-1} glucose. A stepwise increase in the glucose feed rate was executed for simplicity, which closely approximated the exponential feed rate.

Analytical Methods

To determine dry cell weight (DCW), a UV/Vis spectrophotometer (Model DU 640, Beckman, Fullerton, CA) was used to measure the optical density (OD) at 600 nm. Samples were diluted with deionized water to obtain OD readings in the linear range (0 to 0.25 OD units). One-milliliter aliquots of culture medium were centrifuged (8000*g* at 4°C) and resuspended with 1 mL distilled water and dried in preweighed polystyrene microweighing dishes (VWR Scientific, Inc.) at 65°C for 24 h, and weighed. Glucose concentration was measured by a glucose analyzer

(YSI Model 2700, Yellow Springs, OH) with cell free supernatant. On-line GFP fluorescence was measured using a GFP sensor (Randers-Eichhorn et al., 1997) capable of in situ monitoring (DeLisa et al., 1999c). Western blot analysis and enzyme activity assay were performed to obtain the correlation of CAT protein concentration and CAT activity, and their procedures have been described in detail elsewhere (DeLisa et al., 1999c). The specific activity of CAT, 96,900 U mg^{-1}, was used in all simulations.

MODEL DEVELOPMENT

Fed-batch recombinant *E. coli* fermentations are typically carried out in three distinct phases. The first phase is unlimited batch growth in which the cells consume glucose and other nutrients initially present in the fermentation medium. Upon consumption of the initial glucose, the second phase of the process is initiated where additional substrate and/or nutrients are added in a manner that allows high cell concentrations to be obtained. Finally, cloned gene expression is induced by addition of inducer (e.g., promoters such as *lac*, *trc*, *trp*, etc.) or by raising the culture temperature (e.g., λ-based promoters).

A simple model was developed to encompass all three phases for direct implementation of online estimation and optimization algorithms. The model is comprised of mass balance equations for five cultivation components: biomass (X), glucose (S), foreign protein (P_f), inducer (I), and volume (V). For fed-batch fermentation of recombinant *E. coli*, the model was formulated using the following set of equations:

$$\frac{dX}{dt} = \mu X - \frac{X}{V}(F_S + F_I) \tag{1}$$

$$\frac{dS}{dt} = \frac{F_S}{V}(S_F - S) - \frac{\mu X}{Y_{X/S}} - \frac{S}{V}(F_I) \tag{2}$$

$$\frac{dP_f}{dt} = \pi X - k_3 P_f - \frac{P_f}{V}(F_S + F_I) \tag{3}$$

$$\frac{dI}{dt} = \frac{F_I}{V}(I_F - I) - \frac{F_S}{V}(I) - q_I X \tag{4}$$

$$\frac{dV}{dt} = F_S + F_I \tag{5}$$

where μ is the specific growth rate, $Y_{X/S}$ is the biomass yield coefficient, F_S and F_I are the feed rate of glucose and inducer, π is the specific foreign protein production rate, k_3 is the protein degradation rate, and S_F and I_F are the concentrations of glucose and inducer in the feed streams, respectively.

During the batch portion, the specific growth rate can be modeled according to the Monod equation with substrate inhibition (Andrews, 1968). Unfortunately, this equation is inappropriate when foreign protein is expressed. The metabolic burden placed on the cell during recombinant protein production has been well documented (Bentley et al., 1990; Glick, 1995) and is observed macroscopically as a reduction in growth rate (Bentley et al., 1991; Zabriskie et al., 1986). To model the mitigating effect that foreign protein expression has on the specific growth rate, the Monod expression is multiplied by a product inhibition term as follows:

$$\mu = \left[\frac{\mu_{\max} S}{K_S + S + S^2/K_{SI}}\right] \exp(-\alpha P_f) \tag{6}$$

where $\mu_{\max}$ is the maximum specific growth rate, K_S is the substrate saturation constant, K_{SI} is the substrate inhibition constant, and α is a single parameter for growth rate attenuation due to protein expression.

Expression of recombinant protein in *E. coli* is typically performed by amplification of specific messenger RNA via insertion of an inducible promoter located upstream of the foreign gene. One inducible system utilized here is derived from the arabinose operon (*ara* promoter) and is controlled by introduction of arabinose, which, in turn, is also readily metabolized by the cells. Alternatively, the inducible systems derived from the *lac* promoter are regulated by addition of allolactose analogs such as IPTG, a gratuitous, nonmetabolized inducer. Both systems were utilized, although the *ara* promoter system was hypothesized to be more appropriate for process control as the inducer concentration could be both raised (by addition) and decreased (by consumption) with minimal change in biomass concentration (dilution).

A variety of mathematical models have been proposed to describe the cellular kinetics of primary metabolites such as acetate and ethanol. However, there have been few reports of foreign production models that consider induction effects (Bentley et al., 1991; Betenbaugh and Dhurjati, 1990; Lee and Ramirez, 1992; Miao and Kompala, 1992). Lee and Ramirez (1992) proposed a mathematical model that included inducer effects on cell growth and foreign protein production. It successfully described the shock and recovery dynamics of IPTG-induced protein expression on cell growth. For optimization and control studies, simple and more generalized models are required (e.g., Lee and Ramirez, 1992). In some recombinant systems, protein induction is tightly controlled by the presence of strong repressor (*lac*I^q) or by absence of specific polymerase (e.g., T7 systems); however in many systems, the foreign protein is synthesized prior to the addition of inducer via read-through transcription and translation. It is desirable to formulate a model to accommodate both cases, regardless of inducer type (nonmetabolized or metabolized). Two model equations, each with four parameters describing foreign protein expression in *E. coli*, were tested in the present study:

$$\text{Model I: } \pi = k_1 \mu \left(\frac{I}{K_I + I}\right) + k_2 \tag{7}$$

$$\text{Model II: } \pi = k_1\mu\left(\frac{K_{i0}+I}{K_{i1}+I}\right) \tag{8}$$

where k_1 is the induced foreign protein biosynthesis rate, k_2 is the constitutive foreign protein biosynthesis rate, K_I is the induction constant in model I, K_{i0} and K_{i1} are the induction constants in model II. Model I is similar to the model of Leudeking–Piret (Leudeking and Piret, 1959), in which a term for foreign protein induction was included. Model II has been adopted from Bentley et al. (1991) and Lee and Ramirez (1992). To maintain model simplicity, a constant first-order degradation term [k_3 in Eq. (3)] was used in all simulations, as it was a better predictor over a wide range of operating conditions.

Last, for the system using a metabolized inducer (e.g., arabinose), an inducer consumption rate (q_I) was included based on the arabinose uptake mechanisms (Lin, 1996):

$$q_I = q_{I\max}\left[\frac{I}{K_{IC}+I}\right] \tag{9}$$

where q_I is the specific inducer consumption rate, $q_{I\max}$ is the maximum specific consumption rate, and K_{IC} is the saturation constant.

Parameter Estimation

To determine the parameter values, nonlinear regression analysis was performed with an author-written computer program, BIOPARA, based on a constrained optimization technique implemented in a MATLAB optimization toolbox (The Math Works, Inc., Natick, MA). BIOPARA uses the algorithm of sequential quadratic programming (SQP) (Powell, 1983; Schittowski, 1985), in which a quadratic programming (QP) subproblem is solved at each iteration using a line-search method. In the parameter estimation problem, the objective function to minimize is the sum of squared residuals (SSR), which can be defined as follows:

$$\text{Obj} = \text{SSR} = \sum_{j=1}^{m}\sum_{i=1}^{n}\left[(\hat{y}_{i,j} - y_{i,j}) \times W_j\right]^2 \tag{10}$$

where n is the number of observations, m is the number of dependent variables (X, S, and P), $y_{i,j}$ is the ith observed value of the jth dependent variables ($j = 1, \ldots, m$ and $i = 1, \ldots, n$), $\hat{y}_{i,j}$ is the corresponding estimated value from the model equation, and W_j is the weighting factor of the jth variable ($W_j = 1/\overline{y}_j$, where y_j is the arithmetic average value of y_j).

The uncertainty of the parameter estimation was calculated from the mean square fitting error (MSFE) at each estimation (Rosso et al., 1995):

$$\text{MSFE} = \text{SSR}/(n - p) \tag{11}$$

where n is the number of observations and p is the number of parameters being determined.

The parameter values of the proposed model were estimated for each experimental data set. Then, parameter values used in simulation studies were obtained as weight-averaged values of the previously estimated parameters from the different sets of experiments:

$$\overline{\theta}_{\text{weight-averaged}} = \sum_{k=1}^{N}(\theta_k\omega_k)\Big/\sum_{k=1}^{N}(\theta_k) \tag{12}$$

where $\overline{\theta}_{\text{weight-averaged}}$ is the weight-averaged value of the parameter, θ_k is the estimated parameter values using the kth experimental set, ω_k is the weight factor of the parameter estimation for the kth experimental (the weighting factors were selected as 1/MSFE), and N is the total number of experimental sets. Correspondingly, the parameters are listed in Table I, with the approximated 95% confidence interval, calculated as follows:

$$\theta = \overline{\theta}_{\text{weight-averaged}} \pm 1.96\frac{\sigma}{\sqrt{N}} \tag{13}$$

where σ is the standard deviation from the calculation of the average parameter value. The predicted values, $\hat{y}_{i,j}$, were determined by solving the Eqs. (1)–(5) using a third-order Runge–Kutta method with given initial conditions. The SSR value (objective function) was computed at each iteration and the minimum SSR values were obtained for each experimental data set. Note that additional constraints were introduced to assure the optimal parameters occurred in a feasible region. For example, for $Y_{X/S}$, the optimized value must be greater than zero and fall within the range: $0.45 < Y_{X/S} < 0.55$.

RESULTS AND DISCUSSION

Experiments using *E. coli* JM105 [pBAD-GFP::CAT] were performed for estimation of model parameter values and for validating the utility of online GFP monitoring to indicate offline product activity. As noted previously, this *E. coli* strain was employed such that metabolized inducer, arabinose, could be exploited for use in process control.

The growth-related parameters ($\mu_{\max}$, K_S, K_{SI}, and $Y_{X/S}$) were first estimated using the experimenal data (X and S) obtained from four batch cultures (Table I). Among these parameters, K_S was found to have the highest coefficient of variance (CV). Fortunately, this parameter is the least sensitive parameter in the growth model. As noted previously, the parameter values used in simulation and optimization studies were determined by calculating weight-averaged values from each estimated value. The model profiles using the weight-averaged parameters are shown in Figure 1. The predictions were found to fit all sets of batch experimental data reasonably well.

Next, the same algorithm was applied to the production-related parameters (k_1, k_2, k_3, K_I in model I; k_1, K_{i0}, K_{i1}, k_3 in model II). The expression of the fusion proteins was initiated by arabinose induction at optical densities of 75 (fed-batches I and II in Fig. 2) and 125 (fed-batch III in Fig. 2). When all the production-related parameters were esti-

Table I. Estimated values of growth-related parameters in the model for *E. coli* [pBAD-GFP::CAT].

Batch no.	μ_{max} (h^{-1})	K_S (g L^{-1})	K_{SI} (g L^{-1})	$Y_{x/s}$ (g/g)	MSFE	ω_k
1	0.55	0.12	119.10	0.51	0.003	0.400
2	0.53	0.88	76.09	0.54	0.020	0.059
3	0.55	0.15	100.04	0.51	0.003	0.408
4	0.52	0.50	81.12	0.53	0.009	0.133
Weight average[a]	0.55 ± 0.01	0.23 ± 0.30	103.75 ± 16.64	0.52 ± 0.01		
CV (%)[b]	2.12	132.42	16.04	2.06		

[a]Weight average at 95% confidence: $\bar{\theta}_{\text{weight-averaged}} \pm 1.96\,\sigma / \sqrt{N}$.
[b]CV (%): coefficient of variance (%) = error/$\bar{\theta}_{\text{weight-averaged}} \times 100$, where error = $1.96\,\sigma / \sqrt{N}$.

mated simultaneously, several suboptimal sets were found to minimize the SSR, particularly for model I. Subsequently, the values for K_I and $q_{I\max}$ were assumed equal to 0.55 g L^{-1} and 0.005 h^{-1}, respectively, according to DeLisa et al. (1999a), and the value for K_{IC} (0.015 g L^{-1}) was adopted from the literature (Lin, 1996). The remaining production-related parameters (k_1, k_2, k_3, K_{i0}, and K_{i1}) were estimated sequentially based in part on experimental observations. For example, k_2 in model I and k_3 in models I and II, were estimated separately from preinduction, fed-batch phase data, when there was no inducer ($I = 0$) and only constitutive background GFP/CAT production occurred. Other parameters were subsequently estimated using postinduction, fed-batch experimental data. All parameters are summarized in Table II. In Figure 2, the model profiles obtained with estimated parameters and experimental data are compared and both production models (models I and II) fit the data well. Interestingly, in the case of model I, the coefficient of variance (CV) for each parameter was higher than that of model II, so that model II was selected as the foreign protein production model for further analysis.

Once it was discerned that the model could be extended outside the original experimental operating ranges such as induction time and initial glucose concentration, simulations were performed to obtain high protein expression. Results showed that higher levels of recombinant protein were obtained when induction occurred late in exponential growth, although only pulsed additions of inducer were modeled. Consequently, using the simplified foreign protein expression (containing four kinetic parameters that account for the effect of induction), and the standard mass balance equations for a fed-batch reactor, reasonable predictions of cell mass concentration, glucose concentration, and activity of a recombinant product (CAT) were made for a wide range of operating conditions.

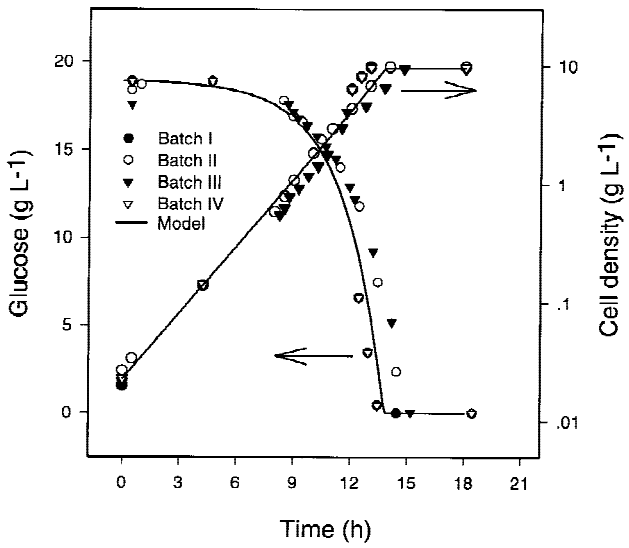

Figure 1. Comparison of model profiles using estimated parameters and experimental data for the growth kinetics of *E. coli* JM105 [pBAD-GFP::CAT]. Time courses of cell density and glucose concentration of all growth phase data are shown. Lines represent model profiles and different symbols represent each experimental set.

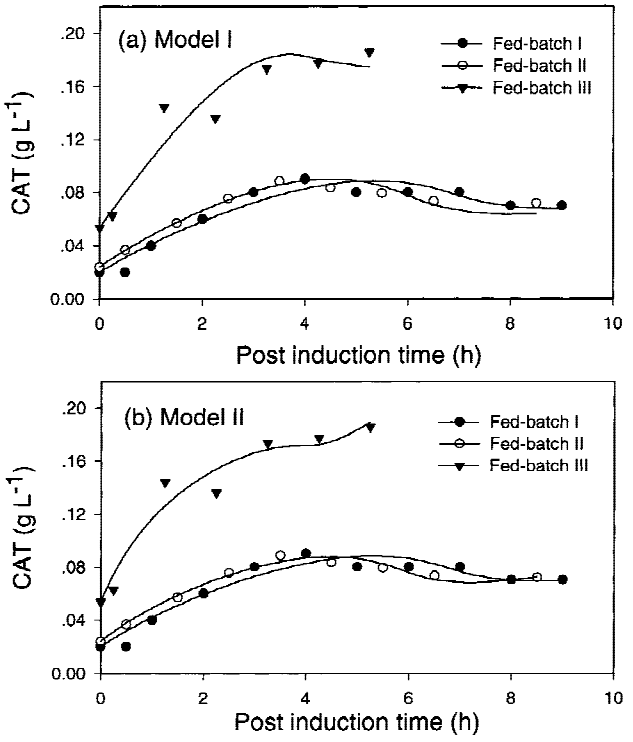

Figure 2. Comparison of model profiles and experimental data using different production models and estimated parameter values. Time courses of foreign protein concentration (CAT) using model I (a) and model II (b) in induced culture of *E. coli* JM105 [pBAD-GFP::CAT]. Lines represent model profiles.

Table II. Estimated parameter values for foreign production model for *E. coli* [pBAD-GFP::CAT].

	Model I					
Exp. no.	k_1 (−)	k_2 (h^{-1})	k_3 (h^{-1})	K_I (g L^{-1})	MSFE	ω_k
1	0.0073	0.00031	0.51	0.55	0.060	0.343
2	0.0045	0.00044	0.72	0.55	0.070	0.297
3	0.0065	0.00054	0.51	0.55	0.057	0.361
Weight average[a]	0.0062 ± 0.0013	0.00043 ± 0.00011	0.60 ± 0.11	0.55 ± 0.00		
CV (%)[b]	18.76	25.50	16.50	0.00		
	Model II					
Exp. no.	k_1 (−)	K_{i0} (g L^{-1})	K_{i1} (g L^{-1})	k_3 (h^{-1})	MSFE	ω_k
1	8.31	0.61	2499.99	0.51	0.028	0.459
2	8.46	0.68	2514.98	0.72	0.030	0.428
3	9.21	0.73	2515.00	0.51	0.112	0.113
Weight average[a]	8.48 ± 0.48	0.65 ± 0.05	2508.1 ± 8.0	0.60 ± 0.11	0.056	
CV (%)[b]	5.67	7.21	0.28	16.50		

[a]Weight average at 95% confidence: $\bar{\theta}_{\text{weight-averaged}} \pm 1.96\,\sigma / \sqrt{N}$.
[b]CV (%): coefficient of variance (%) = error/$\bar{\theta}_{\text{weight-averaged}} \times 100$, where error = $1.96\,\sigma / \sqrt{N}$.

Offline Optimization of Foreign Protein Production in Fed-Batch Cultivation

For design and operation of fed-batch fermentation, it is important to determine the optimal feed rate to maximize productivity. Because there are physical contraints in the operation of fed-batch reactors, the use of a method based on Pontryagins's maximum principle makes it difficult to determine an optimal feeding policy (Wang and Shyu, 1996). In addition, while using the maximum principle, it is necessary to solve highly unstable differential equations during the singular control period (Diener and Goldschmidt, 1994). Moreover, for chemically induced foreign protein production systems, there is the potential for an additional feed rate; that is, inducer feed rate. The performance index (objective function) to be maximized is the total amount of foreign protein:

$$J = \underset{F_S(t),F_I(t)}{\text{Max}} [P_f(t_f)V(t_f)] = \underset{F_S(t),F_I(t)}{-\text{Min}} [P_f(t_f)V(t_f)] \qquad (14)$$

The optimal control problem is to find substrate/inducer feed rate in the time interval: $0 \leq t \leq t_f$. Because expression of foreign proteins can be deleterious to cellular growth, induction was initially off to permit growth to high cell densities until the fed-batch phase. Once dense cultures are reached, addition of inducing agent allows maximal levels of cloned gene expression to be attained. For substrate feeding, an exponential feed rate is commonly used in high cell density (Lee, 1996). Experimentally, a high cell density was accomplished successfully using a feeding policy (DeLisa et al., 1999c), which, in turn, was implemented in our simulated optimization studies. Consequently, the inducer feed rate (F_I) was selected here as a control variable.

The optimal feed profile, $F_I(t)$, and some state variables were subject to the following constraints:

$$0 \leq F_I \leq F_{\text{MAX}} \qquad (15)$$

$$0 \leq V \leq V_{\text{MAX}} \qquad (16)$$

$$0 \leq I \leq I_{\text{MAX}} \qquad (17)$$

To solve this optimal control problem by SQP, the time interval was divided into P stages of equal length:

$$L = \frac{t_f}{P} \qquad (18)$$

A piecewise control policy, $F_I(1), F_I(2), \ldots, F_I(P)$, was sought to maximize the performance index given in Eq. (14). If the P chosen is sufficiently large, a good approximation of the piecewise control to continuous control policy will be obtained. The model parameters and other conditions used in simulations are shown in Table III. In all simulations, substrate feeding profiles were calculated using a constant specific growth rate value ($\mu_{\text{set}} = 0.15\ h^{-1}$) designed to prevent the accumulation of acetic acid (DeLisa et al., 1999a; Han et al., 1992). This would be achieved experimentally using the exponential feed according to Paalme et al. (1990).

As shown in Figure 3, the optimized inducer feeding profiles are similar and are in accordance with previous research (Bentley et al., 1991) in that optimal induction in the midphase of fermentation provided high levels of CAT expression while achieving a high cell density to produce maximal foreign protein. The optimized profile suggests that the greatest amount of inducer (arabinose) should be fed in the middle of the fed-batch phase and later followed by a gradual exponential feed. A comparison of computa-

Table III. Model parameters and other simulation conditions.

Parameter	Strain: JM105 [pBAD-GFP::CAT]	Strain: JM105 [pTH-GFPuv/CAT]	Variable	Strain: JM105 [pBAD-GFP::CAT]	Strain: JM105 [pTH-GFPuv/CAT]
μ_{max} (h^{-1})	0.55	0.36	S_F (g L^{-1})	400	400
K_S (g L^{-1})	0.23	0.13	I_F (g L^{-1})	50	50
K_{SI} (g L^{-1})	103.8	99.0	$X(0)$ (g L^{-1})	0.025	0.025
$Y_{x/s}$ (g/g)	0.52	0.45	$S(0)$ (g L^{-1})	20	20
k_1 (−)	8.48	10.62	$P(0)$ (g L^{-1})	0	0
K_{i0} (g L^{-1})	0.65	27.2	$V(0)$ (g L^{-1})	2	2
K_{i1} (g L^{-1})	2508	2515	S_C (g L^{-1})	0.75	0.75
k_3 (h^{-1})	0.60	0.02	μ_{set} (h^{-1})	0.15	0.15
μ (−)	0.15	0.15	t_f (h)	30	35
q_{Imax} (h^{-1})	0.005	0	F_{MAX} (L h^{-1})	0.5	0.5
K_{IC} (g L^{-1})	0.015	NA[a]	V_{MAX} (L)	4	4

[a]Not applicable.

tional step size ($L = t_f/P$) was made, revealing that the performance index was not significantly increased when L was 1.5 h as compared with a step size of $L = 3.3$ h; however, the computation was threefold faster at $L = 3.3$ h.

In the case of the IPTG induction system (JM105 [pTH-GFPuv/CAT]), a similar optimization analysis was performed with the kinetic parameters estimated analogously (summarized in Table III). The cells grew slightly slower in this case so that the batch phase lasted longer (DeLisa et al., 1999a), and the final time (t_f) was set to 35 h (Fig. 3b). A performance index similar to that of JM105 [pBAD-GFP::CAT] was achieved (PV = 1.088 g). In contrast to the arabinose system, the optimized profile does not suggest additional inducer feeding after the initial pulse, which is likely due to the fact that IPTG is not metabolized.

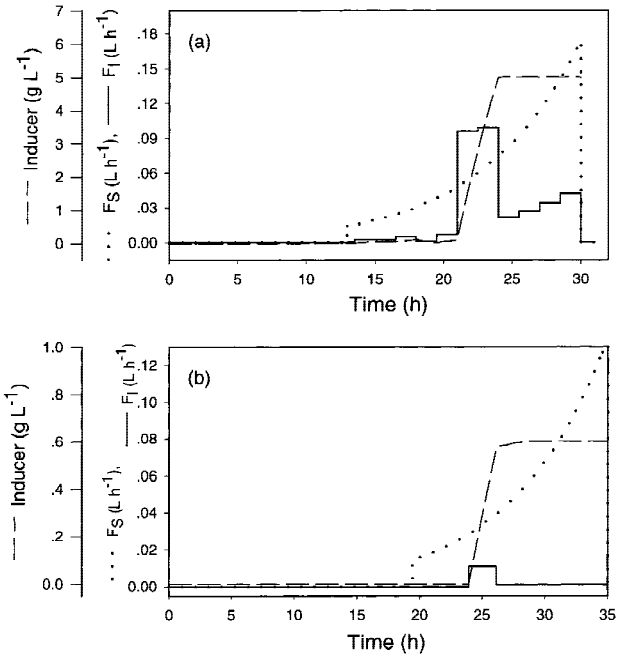

Figure 3. Optimized inducer and substrate feeding control using *E. coli* JM105 [pBAD-GFP::CAT] (a) and *E. coli* JM105 [pTH-GFPuv/CAT] (b).

Several optimization scenarios were run based on constraints commonly observed in laboratory experiments (see Table IV). First, a maximum allowable inducer concentration [I_{MAX} in Eq. (17)] was investigated (constraint type denoted CONC), as per Lee and Ramirez (1992), who noted a significant cost penalty due to added inducer. As the value of I_{MAX} was increased in our simulations, the performance index monotonically increased without apparent limit. Constraining I_{MAX} to within a certain range (0.6 to 1.0 g L^{-1} in the case of IPTG) is consistent with our previous experiments showing that, for IPTG >3.2 m*M* (0.76 g L^{-1}), deleterious metabolic effects were noticed in growth and productivity (Bentley et al., 1991) and, at concentrations >5 m*M*, product expression was erratic and severely inhibited (Harcum et al., 1992).

Second, we specified a constraint on total mass of inducer added to the fermentor (MASS-constrained optimization in Table IV) as follows:

$$I_{MASS} = I_F \times t_f \times \sum_{i=1}^{P} F_I(i) \leq I'_{MAX} \tag{19}$$

This is similar to the concentration constraint, but much more practical both in terms of implementation and in computational efficiency (convergence to the optimum was three to tenfold faster than the CONC-constrained optimization).

Finally, an alternative method for induction policy was proposed (Ramirez and Bentley, 1995) wherein the inducer was included in the glucose feeding solution. In this case, the induction is more gradual and was shown to increase yield. For implementation, the inducer concentration (I_F) to be selected, which is constant in the glucose feed stream, is determined in the optimization. The performance index was lower than previously obtained for inducer feed rate (F_I) control (0.830 g vs. 0.926 g), which was likely due to the fact that this induction strategy did not determine the opti-

Table IV. Optimization results using various conditions.

Inducer	t_f	Control variable	Constraint type	I_{MAX} (g L^{-1}) or I'_{MAX} (g)	Objective function, PV at $t = t_f$ (g)	Volumetric productivity (g L^{-1} h^{-1})	# Iteration	Final volume (L)	Max. inducer conc. (g L^{-1}) or total inducer addition (g)	Optimized I_F (g L^{-1})
Arabinose	30	F_I	CONC	5.0 g L^{-1}	0.926	0.0085	1303	3.62	25.36 g	
				8.0 g L^{-1}	1.385	0.0120	657	3.86	38.16 g	
			MASS	25.0 g	1.065	0.0099	133	3.60	8.17 g L^{-1}	
				30.0 g	1.257	0.0113	133	3.69	9.65 g L^{-1}	
		I_F	CONC	5.0 g L^{-1}	0.830	0.0089	9	3.11	28.85 g	20.91
			MASS	25.0 g	0.690	0.0074	11	3.12	3.99 g L^{-1}	18.02
IPTG	35	F_I	CONC	0.6 g L^{-1}	1.068	0.0100	280	3.04	1.73 g	
				1.0 g L^{-1}	1.539	0.0151	226	2.91	2.90 g	
			MASS	1.7 g	1.118	0.0111	101	2.89	0.79 g L^{-1}	
				2.9 g	1.614	0.0159	17	2.90	1.25 g L^{-1}	
		I_F	CONC	0.6 g L^{-1}	0.947	0.0092	9	2.87	2.05 g	1.98
			MASS	1.7 g	0.845	0.0084	9	2.87	1.73 g L^{-1}	1.66

mal induction time because the inducer was added to the glucose feed and glucose was fed based on a preset policy that maximizes cell mass. That is, this strategy is in part constrained by the glucose feed, as opposed to the previous case where the inducer concentration and addition time were both determined by the optimization algorithm.

In Figure 4, the sensitivity of the performance index to changes in each model parameter is shown, indicating that k_1 was the most important among the seven production-related parameters. This information was used to define parameter selection in on-line parameter estimation simulations.

Online Parameter Estimation

Because GFP fusion constructs were utilized in all the fed-batch experiments, GFP expression was monitored using an on-line sensor for foreign protein concentration. From the linear correlation between online fluorescence intensity and CAT activity (DeLisa et al., 1999c), the foreign protein levels were easily determined using the following linear relationship:

$$P_f(\text{g L}^{-1})|_{t-1.5} = 0.1343 \times FI(V)|_t - 0.0116 \quad (20)$$

where FI is the fluorescence intensity measured in volts by the online GFP sensor. It is known that the GFP fluorescence intensity lags behind the cloned gene expression by approximately 1.5 h due to GFP chromophore cyclization (Albano et al., 1996). Therefore, fluorescence data must be shifted to track the foreign protein level (Albano et al., 1996; DeLisa et al., 1999b).

The optimized inducer feeding profile just obtained is an open loop control, and therefore, it was an offline optimization. It assumed that the state variables proceeded along paths predetermined by the model. A disadvantage of this deterministic approach is that the performance will severely deteriorate in the presence of process disturbances or modeling errors (Vanishsriratana et al., 1997). Online estimation of parameter values, however, can make feedback control strategies possible. In the production model, the protein synthesis parameter, k_1, was the most sensitive parameter in the calculation of the performance index, followed by k_3, the protein turnover rate (see Fig. 4). An online parameter estimator was developed and tested by simulation to ascertain whether key process parameters could be evaluated in real time. The same optimization algorithm (SQP) was used for this online estimation. Because k_1 represents the product protein synthesis rate and GFP fluorescence will be used as a product-monitoring tool, an artificial process disturbance was tracked by online estimation of k_1 (Fig. 5). That is, a disturbance was artificially generated by three sequential step changes in the k_1 during the course of a simulated fermentation in Figure 5a (see Table V). To consider a possible error in GFP expression monitoring and to simulate experimental data closely, errors in a range of ±10% of original values were included in the data using a random

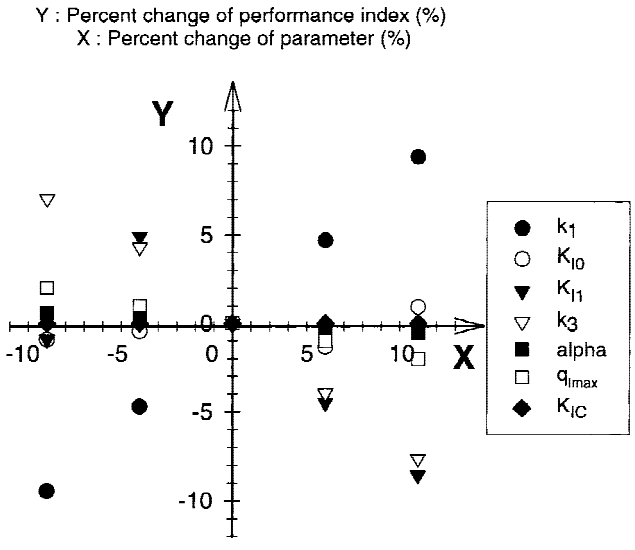

Figure 4. Sensitivity analysis for production-related parameters on performance index (maximum productivity at 30 h) obtained by solving optimal control problem.

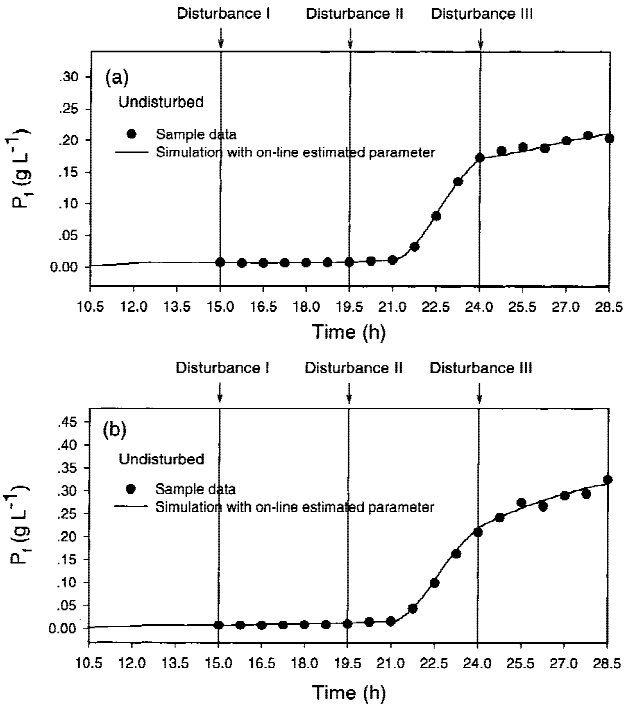

Figure 5. Online parameter estimation results responding to unknown disturbances during the arabinose-induced fermentation. Disturbances were imposed three times (disturbances I, II, and III) during fermentation so that some parameters of the model were changed suddenly. Lines represent the model tracking for sample data subject to the disturbances. Parameter k_1 was changed in (a) and parameters k_1 and k_3 changed in (b) to generate the sample data.

number generator. The original parameter values used in the numerical experiments and the tracked parameter values are shown in Table V. The tracking performance was good and total computation time was <1 min when only seven data points per monitoring window (time interval = 4.5 h) were sampled for the parameter estimation.

In the suboptimal system, it may be unreasonable to expect the disturbance to be solely related to product synthesis (i.e., k_1). To simulate the experimental system more closely, k_3 was also spontaneously changed in a random manner, after which the parameter estimator calculated the k_1 value only (Fig. 5b). In this case, a disturbance was added by step changes in both k_1 and k_3 values as shown in Table V. After the online parameter estimation, k_1 values were much different than the original values (Table V), but the model profiles with these newly estimated parameters still gave a good fit (Fig. 5b), showing good performance of the online parameter estimation.

Table V. On-line parameter estimation results upon arbitrary disturbances.

(a) Change in k_1 only	k_1, original	k_3, original	k_1, estimated
Undisturbed	8.48		NA[a]
Disturbance I	6.36		6.37
Disturbance II	7.96		8.14
Disturbance III	6.11		6.14
(b) Change in k_1 and k_3			
Undisturbed	8.48	0.60	NA
Disturbance I	6.36	0.45	8.07
Disturbance II	9.68	0.54	10.49
Disturbance III	9.96	0.59	10.18

[a]Not applicable.

Online Optimization and Inducer Feed Rate Control

One of our final goals was to use the GFP sensor for development of a process control strategy based on online product levels. One possibility for a model-based control scheme is via generic model control (GMC) (DeLisa et al., 1999b; Lee and Sullivan, 1988). Before applying a control strategy to experimental fementations, the feasibility of a control strategy based on online parameter estimation and optimization using a feedback signal from the GFP probe is demonstrated in Figure 6. First, an open loop optimization was performed leading to an inducer feed profile, denoted F_I^*. According to the offline optimization results, the best inducer feed rate was initiated during the early stage of the fed-batch fermentation (Fig. 6b). With a GFP signal, a 1.5-h time lag has been observed (Albano et al., 1996); hence, the online parameter estimator updated the k_1 parameter from the monitored foreign protein level with a time lag of 1.5 h.

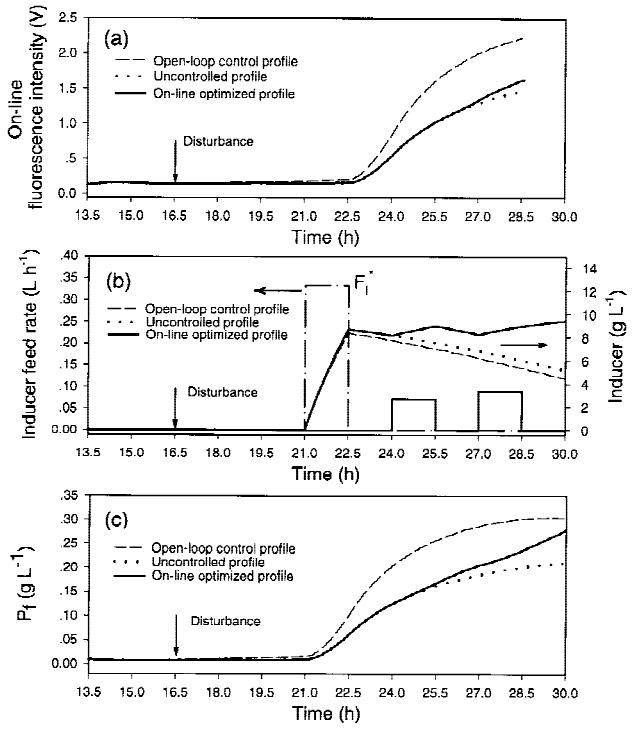

Figure 6. Online optimization of inducer feed rate using GFP signal responding to unknown disturbance imposed at 18 h (arabinose promoter system). The arrow indicates the time of disturbance. Each panel shows online fluorescence intensity from GFP sensor (a), control policies of inducer feed rate (b), and foreign protein concentration profiles (c), respectively.

This updated value was used for the online optimization every 3 h. Thus, at every control interval, the online optimizer integrated the ODEs from the previous step up to the current step using previously estimated parameters. Then, the inducer feed rate for the next step was optimized to maximize the performance index at the next step so that the open loop control (optimized offline) policy was updated with this new optimal solution. In this way, an online optimization and control of inducer feed rate based on feedback signal of GFP was shown.

In the example (Fig. 6), a perturbation was introduced at 16.5 h, which was simulated by a step change in k_1. This is not detectable at the time of the perturbation due to the GFP lag, but results in lower protein expression at the later time periods. After detection of the discrepancy from preoptimized profiles, the control action was evaluated twice, sequentially at 24 h and 27 h, where corrective action in the inducer feed was taken. The computation time was 30 to 60 seconds for the online parameter estimation and 15 seconds for the online optimization. As a result, the online optimizer suggested that additional inducer be fed at each point of control action. Using this feedback control method for evaluating the inducer feed rate, the profile of foreign protein level was improved significantly. This can be seen by noting the separation of the online-optimized trace from the uncontrolled trace (Fig. 6c) and the eventual approach to the open loop solution at the end of the fermentation.

In further simulations, several scenarios approximating common problems found in practice were evaluated. For example, it is well known that, in the absence of a selective marker, plasmid instability can cause a monotonic and accelerating loss of protein expression on a volume basis. This is due to a shift from plasmid-bearing to plasmid-free (nonproducing) cells. We simulated this case by imposing a linear and monotonic decrease in k_1 starting at 18 h ($k_1 = 8.48$) and ending at 30 h ($k_1 = 4.5$). The open loop control profile resulted in 0.3 g/L of protein, which was slightly below the optimal case in Figure 6c. The uncontrolled system, however, yielded 0.15 g/L of protein, whereas the closed-loop online-optimized profile resulted in 0.2 g/L of protein, again demonstrating a net gain by implementing this online optimization framework.

While improvements predicted in these two scenarios were 26% (Fig. 6a) and 33% (plasmid instability), respectively, it is expected that the methodology described here will greatly improve both yield and consistency in run-to-run batches. In addition, the present perturbations, although significant, did not result in catastrophic loss of productivity. Correspondingly, additional scenarios are currently being evaluated that provide a more stringent challenge to this system to determine whether the control methodologies best suited for this system might change.

CONCLUSIONS

A mathematical model describing the expression of recombinant protein in *E. coli* JM105 [pBAD-GFP::CAT] and [pTH-GFPuv/CAT] was developed for the synthesis of operon and translational fusion proteins in batch and fed-batch cultures. A nonlinear regression analysis using an SQP-based algorithm was used to estimate the model parameters. The model was found to be highly accurate while maintaining a simple mathematical structure. Piecewise inducer feed-rate control policies were obtained by solving the optimal control problem using the SQP under different constrained conditions. Among the various optimization conditions tested, MASS-constraint conditions, specifying the maximum limit of inducer amount (mass) provided a rapid convergence. Using the model-based, online parameter estimator, it was possible to update the model parameters to be used in both optimization and process control. Finally, a model based, on-line optimization that uses a simulated feedback signal from a GFP optical sensor to calculate an optimal inducer feed rate was developed.

NOMENCLATURE

CV	coefficient of variance of parameter estimation (%)
F_I	feed rate of inducer (L h^{-1})
F_{MAX}	maximum allowable inducer feed rate (L h^{-1})
F_S	feed rate of substrate (glucose) (L h^{-1})
i	index for observation in an experimental data set (−)
I	inducer concentration (g L^{-1})
I_F	inducer feed concentration (g L^{-1})
I_{MAX}	maximum allowable inducer concentration (g L^{-1})
I'_{MAX}	maximum allowable inducer amount (mass) (g)
j	index for state variable (−)
k	index for experimental data set (−)
k_1	induced biosynthesis rate constant of foreign protein (CAT) (−)
k_2	constitutive biosynthesis rate constant of foreign protein in model I (h^{-1})
k_3	biodegradation rate constant of foreign protein (h^{-1})
K_I	induction constant in foreign protein production model I (g L^{-1})
K_{IC}	Monod constant in inducer consumption model (g L^{-1})
K_S	Monod constant in substrate consumption model (g L^{-1})
K_{SI}	substrate inhibition constant in substrate consumption model (g L^{-1})
K_{i0}	induction constant in foreign protein production model II (g L^{-1})
K_{i1}	induction constant in foreign protein production model II (g L^{-1})
L	time step size in optimal control problem (h)
m	total number of dependent variables in parameter estimation (−)
MSFE	mean squared fitting error
n	total number of observations (−)
N	total number of experimental data set (−)
p	total number of parameters to be determined (−)
P	number of piecewise control steps (−)
P_f	foreign protein (CAT) concentration (g L^{-1})
q_I	specific consumption rate of inducer (h^{-1})
q_{Imax}	maximum specific consumption rate of inducer (h^{-1})
S	substrate (glucose) concentration (g L^{-1})
S_C	critical substrate (glucose) concentration (g L^{-1})
S_F	substrate (glucose) feed concentration (g L^{-1})
SSR	sum of squared residual
t	reaction time (h)
t_f	final time of fermentation (h)
V	culture volume (L)

V_{MAX}	maximum allowable culture volume (L)
W_j	weighting factor of the jth variable
X	cell density (g L^{-1})
y_j	arithmetic average value of y_j
$\hat{y}_{i,j}$	corresponding estimated value from model equation
$y_{i,j}$	the ith observed value of the jth dependent variables
$Y_{X/S}$	biomass yield coefficient (g/g)
α	protein attenuation factor (−)
σ	standard deviation in estimation of average parameter values
θ_k	estimated parameter values using the kth experimental set
$\bar{\theta}_{\text{weight-averaged}}$	weight-averaged parameter value
ω_k	weight factor of the parameter estimation for the kth experimental data set
π	specific foreign protein production rate (h^{-1})
μ	specific growth rate (h^{-1})
μ_{max}	maximum specific growth rate (h^{-1})
μ_{set}	specific growth rate to be set in substrate feed rate calculation (h^{-1})

References

Albano CR, Randers-Eichhorn L, Bentley WE, Rao G. 1998. Green fluorescent protein as a real time quantitative reporter of heterologous protein production. Biotechnol Prog 14:351–354.

Albano CR, Randers-Eichhorn L, Chang Q, Bentley WE, Rao G. 1996. Quantitative measurement of green fluorescent protein expression and chromophore cyclization. Biotechnol Techniq 10:953–958.

Andrews JF. 1968. A mathematical model for the continuous culture of microorganisms utilizing inhibitory substrates. Biotechnol Bioeng 10: 707–723.

Bentley WE, Davis RH, Kompala DS. 1991. Dynamics of CAT expression in *E. coli.* Biotechnol Bioeng 38:749–760.

Bentley WE, Kompala DS. 1989. A novel structured kinetic modeling approach for the analysis of plasmid instability in recombinant bacterial cultures. Biotechnol Bioeng 33:49–61.

Bentley WE, Mirjalii N, Anderson DC, Davis RH, Kompala DS. 1990. Plasmid-encoded protein: the principal factor in the "metabolic burden" associated with recominant bacteria. Biotechnol Bioeng 35: 668–681.

Betenbaugh MJ, Dhurjati P. 1990. A comparison of mathematical model predictions to experimental measurements for growth and recombinant protein production in induced cultures of *Escherichia coli*. Biotechnol Bioeng 36:124–134.

Cha HJ, Dalal NG, Pham MQ, Vakharia V, Bentley WE. 1999a. Insect larval expression process is optimized by generating fusions with green fluorescent protein. Biotechnol Bioeng 65:316–324.

Cha HJ, Pham MQ, Rao G, Bentley WE. 1997. Expression of green fluorescent protein in insect larvae and its application for foreign protein production. Biotechnol Bioeng 56:239–247.

Cha HJ, Wu CF, Valdes JJ, Rao G, Bentley WE. 1999b. Observation of green fluorescent protein as a fusion partner in genetically engineered *Escherichia coli*: monitoring protein expression and solubility. Biotechnol Bioeng 67:565–574.

DeLisa MP. 1999a. An investigation of green fluorescent protein for monitoring and controlling recombinant protein expression in low and high cell density cultivations of *Escherichia coli.* Master's dissertation, University of Maryland, College Park, MD, USA.

DeLisa MP, Chae HJ, Weigand WA, Valdes JJ, Rao G, Bentley WE. 1999b. Generic model control of induced protein expression in high cell density cultivation of *Escherichia coli* using on-line GFP-fusion monitoring. Bioproc Eng. In press.

DeLisa MP, Li J, Rao G, Weigand WA, Bentley WE. 1999c. Monitoring fusion protein expression during high cell density cultivation of *Escherichia coli* using an on-line optical sensor. Biotechnol Bioeng 65: 54–64.

Diener A, Goldschmidt B. 1994. Suboptimal control of fed-batch bioprocesses using phase properties. J Biotechnol 33:71–85.

Domach MM, Shuler ML. 1984. A finite representation model for an asynchronous culture of *E. coli.* Biotechnol Bioeng 26:877–884.

Glick BR. 1995. Metabolic load and heterologous gene expression. Biotechnol Adv 13:247–261.

Han K, Lim HC, Hong J. 1992. Acetic acid formation in *Escherichia coli* fermentation. Biotechnol Bioeng 39:663–671.

Harcum SW, Ramirez DW, Bentley WE. 1992. Optimal nutrient feed policies for heterologous protein production. Appl Biochem Biotechnol 34/35:161–173.

Kleman GL, Chalmers JJ, Luli GW. 1991. A predictive and feedback control algorithm maintains a constant glucose concentration in fed-batch fermentations. Appl Environ Microbiol 57:910.

Lasko DR, Wang DIC. 1996. On-line monitoring of intracellular ATP concentration in *E. coli* fermentations. Biotechnol Bioeng 52:364–372.

Lee PL. 1993. Nonlinear process control: applications of generic model control. London: Springer.

Lee SY. 1996. High cell density culture of *Escherichia coli.* Trends Biotechnol 14:98–105.

Lee PL, Sullivan GR. 1988. Generic model control (GMC). Comput Chem Eng 12:573–580.

Lee J, Ramirez WF. 1992. Mathematical modeling of induced foreign protein production by recombinant bacteria. Biotechnol Bioeng 39: 635–646.

Leudeking R, Piret EL. 1959. A kinetic study of the lactic acid fermentation. J Biochem Microbiol Technol Eng 1:393–412.

Lin ECC. 1996. Dissimilatory pathways for sugars, polyols and carboxylates. In: Neidhardt FC, editors. *Escherichia coli and Salmonella,* 2nd Edition. Vol. 1. Washingtion, DC: ASM Press.

Miao F, Kompala DS. 1992. Overexpression of cloned genes using recombinant *Escherichia coli* regulated by a T7-promoter. 1. Batch cultures and kinetic modeling. Biotechnol Bioeng 40:787–796.

Paalme T, Tiisma K, Kahru A, Vanatalu K, Vilu R. 1990. Glucose-limited fed-batch cultivation of *Escherichia coli* with computer-controlled fixed growth rate. Biotechnol Bioeng 35:312–319.

Powell MJD. 1983. Variable metric methods for constrained optimization. In: Bachem A, Grotschel M, Korte B, editors. Mathematical programming: the state of the art. New York: Springer. p 288–311.

Ramirez DM, Bentley WE. 1995. Fed-batch feeding and induction policies that improve foreign protein synthesis and stability by avoiding stress responses. Biotechnol Bioeng 47:596–608.

Randers-Eichhorn L, Albano CR, Sipior J, Bentley WE, Rao G. 1997. On-line green fluorescent protein sensor with LED excitation. Biotechnol Bioeng 55:921–926.

Riesenberg D. 1991. High cell density cultivation of *Escherichia coli.* Curr Opin Biotechnol 2:380–384.

Rodriguez RL, Tait RC. 1983. Recombinant DNA techniques: an introduction. Menlo Park, CA: Benjamin/Cummings. p 187–191.

Rosso L, Lobry JR, Bajard S, Flandrois JP. 1995. Convenient model to describe the combined effects of temperature and pH on microbial growth. Appl Envrion Microbiol 61:610–616.

Schittowski K. 1985. NLQPL: a FORTRAN subroutine solving constrained nonlinear programming problems. Ann Oper Res 5:485–500.

Schugerl KB, Hitzmann B, Jurgens H, Kullick T, Ulber R, Weigal B. 1996. Challenges in integrating biosensors and FIA for on-line monitoring and control. Trends Biotechnol 14:21–31.

Shimizu N, Fukuzono S, Fujimori K, Nishimura N, Odawara Y. 1988. Fed-batch cultures of recombinant *Escherichia coli* with inhibitory substance monitoring. J Ferment Technol 66:187–191.

Turner C, Gregory ME, Thornhill NF. 1994. Closed-loop control of fed-batch cultures of recombinant *Escherichia coli* using on-line HPLC. Biotechnol Bioeng 44:819–829.

Vanishsriratana W, Zhang BS, Leigh JR. 1997. Optimal control of a fed-batch fermentation process. Trans Inst Meas Control 19:240–251.

Wang FS, Shyu CH. 1996. Optimal feed policy for fed-batch fermentation of ethanol production by *Zymomous mobilis.* Bioproc Eng 17:63–68.

Zabriskie DW, Arcuri EJ. 1986. Factors influencing productivity of fermentations employing recombinant microorganisms. Enzyme Microb Technol 8:705–717.